*

Dynamical Polarization States above the instability threshold for circularly polarized laser emission

C.A. Schrama[†*], M.A. van Eijkelenborg[†], J.P. Woerdman[†], and M. San Miguel[+]
[†]*Huygens Laboratory, Leiden University, P.O. Box 9504, 2300 RA Leiden, The Netherlands*
[+]*Departament de Fisica, Universitat de les Illes Baleares, and*
Instituto Mediterraneo de Estudios Avanzados, IMEDEA (CSIC-UIB)
E-07071 Palma de Mallorca, Spain

(March 27, 1997)

We show that in a laser with a transversally isotropic resonator operating on a J=1→J=0 transition the instability of Circularly Polarized states leads to Linearly Polarized states with a rotating direction of polarization. This transition occurs through intermediate states which are Elliptically Polarized with rotating azimuth. For the range of pump values for which the intermediate Rotating Elliptically Polarized states occur, the total output intensity is constant, and all the energy is pumped into the coherence between the $m_z = 1$ *and* $m_z = -1$ *state.*

Pacs number: 42.55.f

If the pump rate σ of a laser is increased the system eventually crosses a threshold above which it is unstable [1,2]. Above this threshold the output intensity is oscillating. In a laser where the polarization state of the field is not fixed by cavity anisotropies, this boundary can be considerably lower, and not only influences the output intensity but also the state of polarization. Beyond the second threshold a richness of time dependent polarization states can be found [3–7]. In this paper we report on the states occurring beyond this second instability for a laser which for low pump rates emits Circularly Polarized light. The instability leads to states with time dependent polarization properties in which there is simultaneous emission of the two circularly polarized components with equal intensities but with opposite shifts of the optical frequency. The salient feature is that these states are reached, as pumping is increased, through intermediate states for which the total output intensity I is independent of pumping. In these intermediate states the two circularly polarized components of the laser field have different intensities and different frequencies.

Already in the early days of laser physics the polarization state of laser radiation in an isotropic cavity was understood in terms of the angular momentum values of the laser levels [8]. The theory used to describe the lasers was based on third-order Lamb theory. Within this framework most laser transitions could be well described, except for the $J=1 \leftrightarrow J=0$ and the $J=1 \leftrightarrow J=1$ transitions. In the experiments these transitions displayed a certain polarization preference, whereas theory predicted that in a transversally isotropic resonator they should behave neutrally stable; every state of polarization should be possible. Examples of gas lasers operating on these transitions are the HeNe 1.523 μm line [9] and the HeXe 2.652 μm line [10]. The state selection of the $J = 1 \leftrightarrow J = 0$ transition close to the laser threshold was explained [4,8,11] in terms of the ratio γ_c/γ_J, where γ_c is the decay rate of the coherence C between $|J = 1, m_z = 1>$ and $|J = 1, m_z = -1>$ level, and γ_J is the decay rate of the population difference between these two levels. The parameters γ_J and γ_c are more commonly referred to as the relaxation rate of, respectively, the orientation and the alignment of the upper state [12]. If $\gamma_c/\gamma_J > 1$ the laser field is linearly polarized, if $\gamma_c/\gamma_J < 1$ the field is circularly polarized, and if $\gamma_c/\gamma_J = 1$ the field can show any polarization state (neutrally stable). We will focus on the situation $\gamma_c/\gamma_J < 1$, i.e. circular polarization near threshold, since this is the situation that occurs in practice [12]; it is found in all reported experiments on a $J = 1 \leftrightarrow J = 0$ laser transition, including the above mentioned HeNe and HeXe laser lines [9,10]. Recently the $J = 1 \leftrightarrow J = 0$ laser transition has gained renewed interest in the context of dynamical instabilities because of the new phenomena associated with the vectorial properties of the laser field [3–7,13]. The description of the second laser threshold and associated dynamical phenomena requires a theory that goes beyond the third order Lamb theory, taking into account the coupled dynamical equations for the vector electric field and the population levels and coherences of the atomic levels involved in the laser transition. The general problem of polarization state selection has been revisited in this framework and the threshold for the instability of Linearly (LP) and Circularly Polarized (CP) states have been obtained [4]. The situation in which there is preference for LP emission has been analyzed in detail in [5] including the effect of cavity detuning and anisotropies.

---

[*] Present Address: Netherlands Measurements Institute, P.O. Box 654, 2600 AR Delft, The Netherlands

A numerical analysis exploring a variety of time dependent states beyond the second laser threshold has been given in [6].

The basis of the discussion in this paper is given by the set of equations which describe the $J=1 \rightarrow J=0$ laser transition as derived in [4], with the resonator tuned to atomic linecentre and the assumption of a polarization-isotropic resonator. The situation including resonator anisotropies is treated numerically at the end of this paper. For the $J=1$ state there are three decay rates for the three tensor orders of the density matrix of this state. For the $J=0$ state there is only the scalar population which implies only one decay rate. To simplify the discussion it is assumed that the decay rate of the total population of the $J=1$ state and the $J=0$ state is equal, and that there is no spontaneous decay between these two states. Further, the population of the $|J=1, m_{\mathrm{z}}=0>$ state, which is mixed into the dynamics through the collisions, is adiabatically eliminated. The equations of motion in rescaled variables [3] for a cavity resonantly tuned to the atomic frequency are given by

$$\begin{aligned}
\frac{\mathrm{d}E_{\mathrm{R}}}{\mathrm{d}t} &= -\kappa E_{\mathrm{R}} + \kappa P_{\mathrm{R}}, \\
\frac{\mathrm{d}E_{\mathrm{L}}}{\mathrm{d}t} &= -\kappa E_{\mathrm{L}} + \kappa P_{\mathrm{L}}, \\
\frac{\mathrm{d}P_{\mathrm{R}}}{\mathrm{d}t} &= -\gamma_{\perp} P_{\mathrm{R}} + \gamma_{\perp} E_{\mathrm{R}} \frac{D_{+}+D_{-}}{2} + \gamma_{\perp} E_{\mathrm{L}} C, \\
\frac{\mathrm{d}P_{\mathrm{L}}}{\mathrm{d}t} &= -\gamma_{\perp} P_{\mathrm{L}} + \gamma_{\perp} E_{\mathrm{L}} \frac{D_{+}-D_{-}}{2} + \gamma_{\perp} E_{\mathrm{R}} C^{*}, \\
\frac{\mathrm{d}C}{\mathrm{d}t} &= -\gamma_{\mathrm{c}} C - \frac{\gamma_{\|}}{4}\left(E_{\mathrm{L}}^{*} P_{\mathrm{R}} + E_{\mathrm{R}} P_{\mathrm{L}}^{*}\right), \\
\frac{\mathrm{d}D_{+}}{\mathrm{d}t} &= -\gamma_{\|}(D_{+} - 2\sigma) - \frac{3\gamma_{\|}}{2} \mathrm{Re}\left(E_{\mathrm{R}}^{*} P_{\mathrm{R}} + E_{\mathrm{L}}^{*} P_{\mathrm{L}}\right), \\
\frac{\mathrm{d}D_{-}}{\mathrm{d}t} &= -\gamma_{\mathrm{J}} D_{-} - \frac{\gamma_{\|}}{2} \mathrm{Re}\left(E_{\mathrm{R}}^{*} P_{\mathrm{R}} - E_{\mathrm{L}}^{*} P_{\mathrm{L}}\right),
\end{aligned} \tag{1}$$

where E_{R} and E_{L} are the right and left circularly polarized complex field amplitudes, P_{R} and P_{L} are the amplitudes of dipole moments on the circularly polarized transitions, C is the coherence between the $m_{\mathrm{z}}=1$ and $m_{\mathrm{z}}=-1$ state, and $(D_{+} \pm D_{-})/2$ is the inversion on the right/left circularly polarized transition; κ is the cavity decay rate [14], $\gamma_{\perp}$ is the decay rate of the atomic dipole moment and $\gamma_{\|}$ is the population decay rate.

Above the laser threshold $\sigma=1$ these equations have steady state solutions as discussed above [4]. There is a CP solution in which either $I_{\mathrm{R}}=|E_{\mathrm{R}}|^2=0$ or $I_{\mathrm{L}}=|E_{\mathrm{L}}|^2=0$ and a LP solution with $I_{\mathrm{R}}=I_{\mathrm{L}}$. In both solutions the field amplitudes are resonantly tuned to the atomic frequency. For CP solutions there is bistability between right and left polarization, while for the LP solution the polarization angle is undetermined. A linear stability analysis of these solutions indicates that, close to threshold, CP is stable for $\gamma_{\mathrm{c}}/\gamma_{\mathrm{J}}<1$, while LP is stable for $\gamma_{\mathrm{c}}/\gamma_{\mathrm{J}}>1$. The case $\gamma_{\mathrm{c}}/\gamma_{\mathrm{J}}=1$ is 'neutral' and any Elliptically Polarized (EP) state in which two polarization components coexist is possible: The ellipticity defined as $\tan\chi = (|E_{\mathrm{R}}|-|E_{\mathrm{L}}|)/(|E_{\mathrm{R}}|+|E_{\mathrm{L}}|)$ takes on arbitrary values and the azimuth giving the orientation of the dominant linearly polarized component is undetermined. The linear stability analysis also identifies the second laser threshold as the critical value of the pump rate above which these particular solutions are unstable. A Hopf bifurcation occurs at the critical pump rate given by [4]

$$\sigma_1 = 1 + \frac{n_{\mathrm{gr}}\gamma_{<}(\kappa+\gamma_{\perp}+\gamma_{<})(3\gamma_{>}+\gamma_{\|})}{\gamma_{\|}\left[2\kappa(\kappa+\gamma_{\perp})+\gamma_{>}(\kappa-\gamma_{<}-\gamma_{\perp})\right]}, \tag{2}$$

where $\gamma_{<}$ is the smaller of γ_{c} and γ_{J}, and $\gamma_{>}$ is the larger of γ_{c} and γ_{J}. The group index n_{gr} is given by $1+\kappa/\gamma_{\perp}$. The total intensity $I=I_{\mathrm{R}}+I_{\mathrm{L}}$ at this critical value can be found from

$$I = 4\gamma_{>}(\sigma-1)/(3\gamma_{>}+\gamma_{\|}). \tag{3}$$

Above σ_1 this symmetric description ceases to hold. For $\gamma_{\mathrm{c}}/\gamma_{\mathrm{J}}>1$ the total intensity and the ellipticity oscillate anharmonically [4,5]. In this paper we focus on the case $\gamma_{\mathrm{c}}/\gamma_{\mathrm{J}}<1$ for which a rather different behaviour with time independent total intensity is found. Guided by numerical phenomenology [6] we search for steady state solutions of Eq. (1) which involve two frequencies in the form

$$\begin{aligned}
E_{R,L} &= \epsilon_{R,L} e^{\mp i\Omega_{R,L} t}, \\
P_{R,L} &= p_{R,L} e^{\mp i\Omega_{R,L} t}, \\
C &= c e^{-i(\Omega_{\mathrm{R}}+\Omega_{\mathrm{L}})t}.
\end{aligned} \tag{4}$$

One then finds

$$\left(\sigma - 1 + \frac{\Omega_{\mathrm{R}}^2}{\gamma_{\perp}\kappa} - \frac{3}{4}(I_{\mathrm{R}}+I_{\mathrm{L}}) - \frac{\gamma_{\|}}{4\gamma_{\mathrm{J}}}(I_{\mathrm{R}}-I_{\mathrm{L}}) - \frac{\gamma_{\|}}{4\kappa}\frac{2\kappa\gamma_{\mathrm{c}}+(\Omega_{\mathrm{R}}+\Omega_{\mathrm{L}})^2}{\gamma_{\mathrm{c}}^2+(\Omega_{\mathrm{R}}+\Omega_{\mathrm{L}})^2} I_{\mathrm{L}}\right) I_{\mathrm{R}} = 0, \tag{5a}$$

$$\left(\sigma - 1 + \frac{\Omega_{\mathrm{L}}^2}{\gamma_{\perp}\kappa} - \frac{3}{4}(I_{\mathrm{R}}+I_{\mathrm{L}}) + \frac{\gamma_{\|}}{4\gamma_{\mathrm{J}}}(I_{\mathrm{R}}-I_{\mathrm{L}}) - \frac{\gamma_{\|}}{4\kappa}\frac{2\kappa\gamma_{\mathrm{c}}+(\Omega_{\mathrm{R}}+\Omega_{\mathrm{L}})^2}{\gamma_{\mathrm{c}}^2+(\Omega_{\mathrm{R}}+\Omega_{\mathrm{L}})^2} I_{\mathrm{R}}\right) I_{\mathrm{L}} = 0, \tag{5b}$$

and

$$\left(\Omega_{\mathrm{R}} n_{\mathrm{gr}} - \frac{\gamma_{\|}}{4}\frac{(2\kappa-\gamma_{\mathrm{c}})(\Omega_{\mathrm{R}}+\Omega_{\mathrm{L}})}{\gamma_{\mathrm{c}}^2+(\Omega_{\mathrm{R}}+\Omega_{\mathrm{L}})^2} I_{\mathrm{L}}\right) I_{\mathrm{R}} = 0, \tag{6a}$$

$$\left(\Omega_{\mathrm{L}} n_{\mathrm{gr}} - \frac{\gamma_{\|}}{4}\frac{(2\kappa-\gamma_{\mathrm{c}})(\Omega_{\mathrm{R}}+\Omega_{\mathrm{L}})}{\gamma_{\mathrm{c}}^2+(\Omega_{\mathrm{R}}+\Omega_{\mathrm{L}})^2} I_{\mathrm{R}}\right) I_{\mathrm{L}} = 0. \tag{6b}$$

Eqs. (6) admit several solutions which obviously include the ones known to be stable for $\sigma<\sigma_1$. It follows from (6) that if $I_{\mathrm{R}}=0$ then $\Omega_{\mathrm{L}}=0$, and if $I_{\mathrm{L}}=0$ then $\Omega_{\mathrm{R}}=0$. These two cases correspond to the left and right CP solutions described above. If both $I_{\mathrm{R}}\neq 0$ and $I_{\mathrm{L}}\neq 0$ then either $\Omega_{\mathrm{R}}=\Omega_{\mathrm{L}}=0$, or $\Omega_{\mathrm{R}}\neq 0$ and $\Omega_{\mathrm{L}}\neq 0$. The first case corresponds to the, above described, LP solutions. The last case corresponds to the new solutions we are looking for. We will distinguish two cases: $I_{\rm R}=I_{\rm L}$ with $\Omega_{\rm R}=\Omega_{\rm L}$ (Rotating LP, RLP), and $I_{\rm R}\neq I_{\rm L}$, (Rotating EP, REP).

Before discussing these two types of solutions we first give a relation valid in both cases. By adding Eqs. (6) one finds

$$(\Omega_{\rm R}+\Omega_{\rm L})^2=\frac{\gamma_{\|}(2\kappa-\gamma_{\rm c})}{4n_{\rm gr}}(I_{\rm R}+I_{\rm L})-\gamma_{\rm c}^2. \qquad (7)$$

This equation reveals that these solutions can only exist if $2\kappa>\gamma_{\rm c}$. This condition can be called the polarization bad cavity condition [15].

Rotating Linear Polarization, RLP: $I_{\rm R}=I_{\rm L}=I/2$, $\Omega_{\rm R}=\Omega_{\rm L}=\Omega$. In these solutions the two circularly polarized components of the field coexist with equal strength, which corresponds to a linearly polarized field whose angle of polarization (azimuth) is given by the phase difference of the two complex amplitudes. Here the phase difference is given by $2\Omega t$, which implies a rotation of the polarization direction with frequency 2Ω. From Eqs. (5) and (6) one immediately obtains that

$$I=4n_{\rm gr}\left\{\frac{4\kappa\gamma_{\perp}(\sigma-1)-\gamma_{\rm c}(\gamma_{\rm c}+2\kappa+2\gamma_{\perp})}{12\kappa(\kappa+\gamma_{\perp})+\gamma_{\|}(\gamma_{\rm c}+2\gamma_{\perp})}\right\}. \qquad (8)$$

The frequency Ω is easily obtained replacing (8) in (7). The requirements that $I>0$ and $\Omega^2>0$ identify the range of pump rates for which these solutions exist. The condition giving a higher pump rate is $\Omega^2>0$, implying that RLP solutions only exist for $\sigma>\sigma_0$, where

$$\sigma_0=1+\frac{\gamma_{\rm c}(3\gamma_{\rm c}+\gamma_{\|})n_{\rm gr}}{\gamma_{\|}(2\kappa-\gamma_{\rm c})}. \qquad (9)$$

In practical cases $\sigma_0<\sigma_1$ [16] so that there is a range of pump rates in which the CP states are stable and for which RLP states already exist. However, as we see next, the RLP states are stable only for $\sigma>\sigma_2$ and the system chooses not to switch from CP to RLP with a discontinuity in the value of $I_{\rm R}$ and $I_{\rm L}$, but rather the transition from CP to RLP appears mediated with continuity through REP states.

Rotating Elliptical Polarization, REP: $I_{\rm R}\neq I_{\rm L}$ and $\Omega_{\rm R}\neq\Omega_{\rm L}$. The two circularly polarized components coexist with unequal but time independent strength. This gives rise to an EP state with time independent ellipticity. However, the azimuth of the ellipse is given by the phase difference of the two complex amplitudes and therefore it rotates with frequency $\Omega_{\rm R}+\Omega_{\rm L}$. The total intensity and rotating frequency is obtained from Eqs. (5) and (6). It follows from the difference of Eq. (5a) and Eq. (5b), while using Eqs. (6) and (7), that

$$I=I_{\rm R}+I_{\rm L}=\frac{4\gamma_{\rm c}\gamma_{\rm J}(\kappa+\gamma_{\perp}+\gamma_{\rm c})n_{\rm gr}}{\gamma_{\|}\left[2\kappa(\kappa+\gamma_{\perp})+\gamma_{\rm J}(\kappa-\gamma_{\rm c}-\gamma_{\perp})\right]}. \qquad (10)$$

Substituting Eq. (10) into Eq. (7) yields

$$(\Omega_{\rm R}+\Omega_{\rm L})^2=\frac{2\kappa\gamma_{\rm c}(\gamma_{\rm J}-\gamma_{\rm c})(\kappa+\gamma_{\perp})}{2\kappa(\kappa+\gamma_{\perp})+\gamma_{\rm J}(\kappa-\gamma_{\rm c}-\gamma_{\perp})}. \qquad (11)$$

Note that I coincides with the intensity at the instability threshold σ_1 for the CP solutions and that it is independent of pump rate. Note also that $(\Omega_{\rm R}+\Omega_{\rm L})^2$ coincides with the frequency of the Hopf bifurcation at this threshold [4] and it is also independent of pump rate. The existence of these solutions require $(\Omega_{\rm R}+\Omega_{\rm L})^2>0$ which is fulfilled for $\gamma_{\rm J}>\gamma_{\rm c}$ and $I>0$, but it also requires $I_{\rm R}>0$ and $I_{\rm L}>0$. For the latter conditions we see that from the sum of Eq. (5a) and Eq. (5b) one finds

$$\cos^2(2\chi)=(\sigma-1)\frac{2\left[2\kappa(\kappa+\gamma_{\perp})+\gamma_{\rm J}(\kappa-\gamma_{\rm c}-\gamma_{\perp})\right]}{\gamma_{\rm c}(\gamma_{\rm J}-\gamma_{\rm c})n_{\rm gr}} -\frac{2(\gamma_{\|}+3\gamma_{\rm J})(\gamma_{\perp}+\gamma_{\rm c}+\kappa)}{\gamma_{\|}(\gamma_{\rm J}-\gamma_{\rm c})}. \qquad (12)$$

Solving $\cos^2(2\chi)=0$ and $\cos^2(2\chi)=1$ with $\gamma_{\rm J}>\gamma_{\rm c}$ gives the range of pump rates of existence of REP solutions. The first condition reproduces the instability threshold Eq. (2), while the second identifies another threshold value

$$\sigma_2=\sigma_1+\frac{\gamma_{\rm c}(\gamma_{\rm J}-\gamma_{\rm c})n_{\rm gr}}{2\left[2\kappa(\kappa+\gamma_{\perp})+\gamma_{\rm J}(\kappa-\gamma_{\rm c}-\gamma_{\perp})\right]}. \qquad (13)$$

At $\sigma=\sigma_1$ the CP solution coincides with a REP solution and in turn, this coincides with the RLP solution at $\sigma=\sigma_2$. The individual frequencies $\Omega_{\rm R}$ and $\Omega_{\rm L}$ for these solutions can be found from Eqs. (6) while using the identity $I_{\rm R}=I(1+\sin(2\chi))/2$.

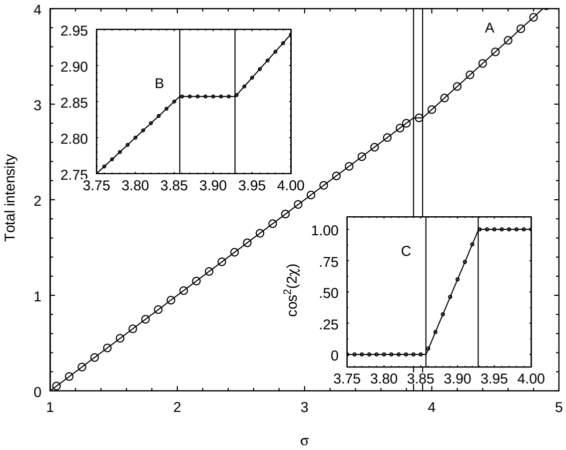

FIG. 1. A,B: total intensity versus σ. The inset B is an enlargement of the transition region. The inset C shows $\cos^2(2\chi)$ versus σ. These plots have been made with the parameters $\kappa=\gamma_{\|}=\gamma_{\rm J}=\gamma_{\perp}=1$ and $\gamma_{\rm c}=0.5$ [17].

The behaviour of the laser in the transition from CP to RLP states is shown in Fig. 1, where the total intensity as function of σ has been plotted. For $\sigma<\sigma_1$, $\sigma_1<\sigma<\sigma_2$ and $\sigma>\sigma_2$ the intensity I is calculated from Eq. (3), Eq. (10) and Eq. (8) respectively. A plateau in I appears between the vertical lines which correspond to σ_1 and

σ_2. In the insets the transition region has been enlarged. In B, again, I as function of σ has been plotted. In C $\cos^2(2\chi)$ versus σ is drawn as calculated for $\sigma_1 < \sigma < \sigma_2$ from Eq. (12). The latter inset shows the change in ellipticity during this transition, going from a circle to a line as degenerate cases of the ellipse. In all three plots the circles are results of numerical integrations of Eqs. (1). Note that $\mathrm{d}I/\mathrm{d}\sigma$ is different before, during, and after the transition. In the CP state (stable for $\sigma < \sigma_1$) the total intensity, which equals the intensity of the nonvanishing component of the field, grows linearly with σ and with unit slope (for the parameters noted in the caption of Fig. 1). In the RLP solution (stable for $\sigma > \sigma_2$), the intensity of both components also grows linearly with a slope smaller than 1, but the total intensity has a slope larger than 1. This solution has an unstable branch with the same slope for $\sigma < \sigma_2$ down to $\sigma = \sigma_0$ where the solution disappears.

During the transition region ($\sigma_1 < \sigma < \sigma_2$) the total intensity does not depend on σ (see Eq. (10)). Therefore during the transition from CP to RLP states the total intensity has zero slope, while the intensities of the two components giving rise to these REP states grow and decrease with $\sqrt{\sigma}$ to become equal at $\sigma = \sigma_2$. The energy pumped into the laser for $\sigma_1 < \sigma < \sigma_2$ does not result in higher output power but it goes into the atomic coherences.

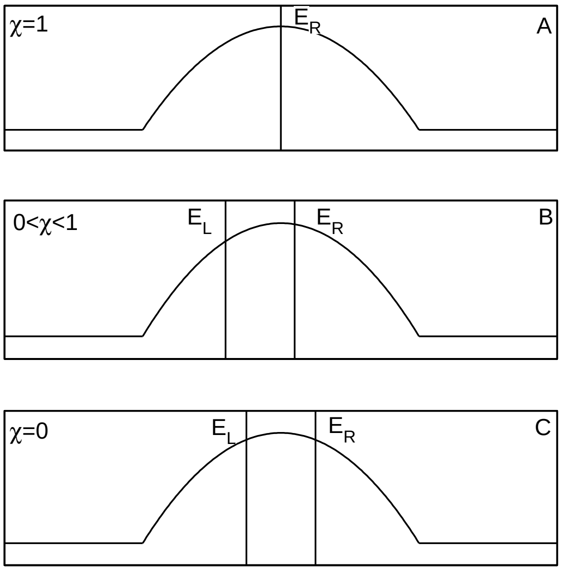

FIG. 2. Mode frequencies with respect to the gain profile. A: $\sigma \leq \sigma_1$; B: $\sigma_1 < \sigma < \sigma_2$; C: $\sigma \geq \sigma_3$.

The emergence of laser states with time dependent polarization properties, while keeping a total intensity constant, is possible because of the existence of only two frequencies in the dynamical solution. In general two frequencies give rise to polarization selfpulsations as it becomes evident if the RLP or REP solutions are described in terms of the linear components E_x and E_y of the field ($E_\pm = (E_\mathrm{x} \pm iE_\mathrm{y})/\sqrt{2}$). The intensities of the x- and y-components become periodic in time. In our problem the circular components are the natural basis in which the emergence of two frequencies can be easily understood as visualized in Fig. 2 where the mode frequencies with respect to the gain profile are shown. For $\sigma \leq \sigma_1$ only one mode is lasing. For $\sigma_1 < \sigma < \sigma_2$ both circular modes are lasing . They are however not equally detuned with respect to gain maximum. This causes the elliptical polarization. For $\sigma > \sigma_2$ the modes are equally detuned, hence the field is RLP.

The polarization time dependent states which we have found beyond the instability of CP states admit an interesting representation on a Poincaré sphere (Fig. 3) which is parametrized by the two relevant polarization angles, ellipticity and azimuth. The two poles of the sphere describe the two CP states. A point in the equator is a linearly polarized state with direction of polarization given by the azimuth on the equator. An arbitrary point in the sphere corresponds to an elliptically polarized state. The point on the pole becomes unstable for $\sigma > \sigma_1$ and for $\sigma > \sigma_2$ ends on a point that circles the sphere along the equator (RLP). The intermediate states in this transition are states in which the representative point rotates along a parallel circle with a frequency $\Omega_\mathrm{R} + \Omega_\mathrm{L}$ (REP). The rotating frequency at $\sigma = \sigma_1$ is the frequency of the Hopf bifurcation in which the point in the pole becomes unstable.

In summary, we have analyzed a laser operating on a $J = 1 \rightarrow J = 0$ transition under the conditions of polarization bad cavity ($2\kappa > \gamma_\mathrm{c}$) and preference to start lasing with circularly polarized states ($\gamma_\mathrm{J} > \gamma_\mathrm{c}$). In these circumstances there is a Hopf bifurcation of the CP states. Beyond this bifurcation at $\sigma = \sigma_1$ there appear states with time dependent polarization properties characterized by two frequencies and constant total intensity. The instability leads from CP states to LP states with a rotating direction of polarization. This transition occurs continuously through intermediate states which are EP with rotating azimuth. For the range of pump values $\sigma_1 < \sigma < \sigma_2$ for which the intermediate REP states occur, the total output intensity is independent of pump rate. The frequency of rotation of the ellipse is also constant and it is given by the Hopf frequency at the instability point.

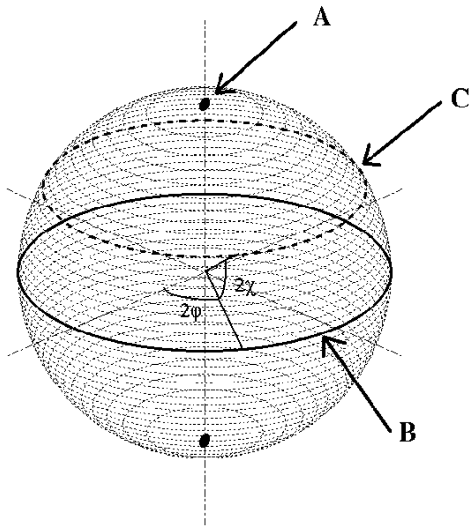

FIG. 3. Poincaré sphere representation of polarization states. A) Pole: Circularly Polarized (CP), B) Parallel Circle: Rotating Elliptically Polarized (REP), C) Equator:Rotating Linearly Polarized (RLP).

Experimental work on the $J=1 \rightarrow J=0$ transition is of great importance since this transition is the only transition for which the rigorous laser models can be handled. In our theoretical treatment we have assumed an isotropic resonator. However, practical laser resonators always contain some residual anisotropies. In principle, these can be cancelled by adding intentional intracavity anisotropies of opposite sign. However, since such cancellation is never perfect one might still worry whether the presence of anisotropies would spoil the theoretical results reported in this paper. We have therefore investigated the effects of linear dichroism α and linear birefringence β ($\alpha, \beta \ll \kappa$) by numerical integration of Eqs. (1) in the same manner as was done in ref. [5]. This gives the following results. Just above threshold ($\sigma \gtrsim 1$) a dichroism α induces linearly polarized steady state solutions, whereas a birefringence β induces oscillations in the ellipticity χ. Further above threshold (but still below σ_1) the influence of the medium on the polarization becomes stronger, and the steady states become identical to the states found without anisotropies (CP). Above the threshold σ_1 both α and β induce small oscillations in both χ and I. The time-averaged behavior is still given by the above polarization isotropic situation (Fig. 1). The modulation depth of the oscillations in χ and I is roughly of the order of $|\alpha+i\beta|$ (which experimentally can be brought to below 10^{-4} [18]). Thus, although residual anisotropies induce small oscillations around the steady state for values of $\sigma > \sigma_1$, the oscillations remain very small and the time averaged behavior of the laser is unaffected. Therefore our theoretical results may be expected to be valid in practical cases.

Additional motivation for the work on the non-linear dynamics of gas lasers is recent work on VCSELs (Vertical Cavity Surface Emitting Lasers) [19,20]. In order to avoid condensed matter complexity, existing theory for polarization behaviour of VCSELs is structured along the lines of gas laser theory [21]. Questions in relation to such VCSEL theory and its improvement may be elucidated by the gas-laser results.

This work is part of the research program of the "Stichting voor Fundamenteel Onderzoek der Materie (FOM)". We acknowledge financial support from the European Union under the ESPRIT project 20029 ACQUIRE and the TMR Network ERB4061PL951021. We are grateful for helpful discussions of this problem with N.B. Abraham.

---

[1] A. Grasyuk and A.N. Oraevsky, in Quantum Electronics and Coherent light, P.A. Miles and C.H. Townes, eds. (Academic Press, New York 1964) p. 192.
[2] H. Haken, Z. Phys. 190 (1966) 327.
[3] G.P. Puccioni, M.V. Tratnik, J.E. Sipe, and G.L. Oppo Opt. Letters 12 (1987) 242.
[4] N.B. Abraham, E. Arimondo, and M. San Miguel, Opt. Commun. 117 (1995) 344; Note that the correct values for the instability threshold σ_1 are given in *ibid.* 121 (1995) 168.
[5] M.D. Matlin, R.S. Gioggia, N.B. Abraham, P. Glorieux, and T. Crawford, Opt. Commun. 120 (1995) 204.
[6] N.B. Abraham, M.D. Matlin, and R.S Gioggia, Phys. Rev. A 53 (1996) 3514.
[7] J.Redondo, E. Roldan and G.J. de Valcarcel, Phys. Lett. A 210 (1996) 301.
[8] W. van Haeringen, Phys Rev 158 (1967) 256.
[9] W.J. Tomlinson and R.L. Fork, Phys. Rev. 164 (1967) 466; H. de Lang and G. Bouwhuis, Phys. Lett. 20 (1966) 383; W.J. Tomlinson and R.L. Fork, Phys. Rev. Lett. 20 (1968) 647.
[10] W. Culshaw and J. Kannelaud, Phys. Rev. 156 (1967) 308.
[11] D. Lenstra, Phys. Rep. 59 (1980) 299.
[12] C.H. Wang and W.J. Tomlinson, Phys. Rev. 181 (1969) 115.
[13] C. Serrat, A. Kul'minskii, R. Vilaseca and R. Corbalan, Opt. Lett. 20 (1995) 1353; A. Kul'minskii, R. Vilaseca and R. Corbalan, Opt. Lett. 20 (1995) 2390.
[14] Note that this is the amplitude decay rate; the decay rate of the intensity is 2κ.
[15] C.A. Schrama, M.A. van Eijkelenborg and J.P. Woerdman, Opt. Commun. 132 (1996) 557.
[16] This is the case for most reasonable parameter values. A sufficient requirement is that $\gamma_c + \gamma_\perp > \kappa$ when $\gamma_J > \gamma_c$.
[17] Although the chosen parameters may have somewhat unlikely values, they are merely used as an example of very generic behaviour.
[18] M.A. van Eijkelenborg, C.A. Schrama, and J.P. Woerdman, Opt. Commun. 119 (1995) 97.

[19] A.K. Jansen van Doorn, M.P. van Exter, M. Travagnin, and J.P. Woerdman, Optics Comm. 133 (1997) 252.
[20] A.K. Jansen van Doorn, M.P. van Exter, and J.P Woerdman, Appl. Phys. Lett. 69 (1996) 1041.
[21] M. San Miguel, Q. Feng, and J.V. Moloney, Phys. Rev. A 52 (1995) 1728. J. Martin-Regalado, M. San Miguel, N.B. Abraham and F. Prati. Opt. Lett. 21 (1996) 351; J. Martin-Regalado, F. Prati, M. Sanmiguel and N.B. Abraham, to be published in IEEE J. Quant. Electron.